High Performance Patch Antenna using Circular Split Ring Resonators and Thin Wires Employing Electromagnetic Coupling Improvement

Abdelrehim, Adel Amin Abouelhamd; Ghafouri-Shiraz, Hooshang

DOI:
10.1016/j.photonics.2016.05.002

Document Version
Peer reviewed version

Citation for published version (Harvard):
Abdelrehim, AAA & Ghafouri-Shiraz, H 2016, 'High Performance Patch Antenna using Circular Split Ring Resonators and Thin Wires Employing Electromagnetic Coupling Improvement', *Photonics and Nanostructures - Fundamentals and Applications*, vol. 21, pp. 19-31. https://doi.org/10.1016/j.photonics.2016.05.002

ELSEVIER

High Performance Patch Antenna using Circular Split Ring Resonators and Thin Wires Employing Electromagnetic Coupling Improvement

Adel A. A. Abdelrehim and H. Ghafouri-Shiraz

School of Electronic, Electrical and System Engineering, University of Birmingham, Birmingham, B15 2TT, United Kingdom

Elsevier use only: Received date here; revised date here; accepted date here

Abstract

In this paper, three dimensional periodic structure composed of circular split ring resonators and thin wires is used to improve the performance of a microstrip patch antenna. The three dimensional periodic structure is placed at the top of the patch within a specific separation distance to construct the proposed antenna. The radiated electromagnetic waves intensity of the proposed antenna is improved compared with the conventional patch antenna due to the electric and magnetic coupling enhancements. These enhancements occur between the patch and the periodic structure resonators and between the different resonator pairs of the periodic structure. As a result, the electric and the magnetic fields at the top of the patch are improved, the radiated electromagnetic beam size reduces which results in a highly focused beam and hence the antenna directivity and gain are improved, while the beam are is reduced. The proposed antenna has been designed and simulated using CST microwave studio at 10 GHz. An infinite two dimensional periodicity unit cell of circular split ring resonator and thin wire is designed to resonate at a 10 GHz and simulated in CST software, the scattering parameters are extracted, the results showed that the infinite periodicity two dimensional structure has a pass band frequency response of good transmission and reflection characteristics around 10 GHz. The infinite periodicity of the two dimensional periodic structure is then truncated and multi layers of such truncated structure is used to construct a three dimensional periodic structure. A parametric analysis has been performed on the proposed antenna incorporated with the three dimensional periodic structure. The impacts of the separation distance between the patch and three dimensional periodic structures and the size of the three dimensional periodic structure on the radiation and impedance matching parameters of the proposed antenna are studied. For experimental verification, the proposed antenna operating at 10 GHz is fabricated; the return loss and the gain for the proposed antenna with and without metamaterial are measured. Furthermore, the results show that, the antenna gain is improved by 4.6 dB while the beam width is reduced from 75 degrees to 41 degrees which validate the concept of beam focusing using electromagnetic coupling between the patch and the three dimensional periodic structure and between the different unit cells of the periodic structure, and also the return loss is improved by -20 dB, while the bandwidth is slightly reduced. The simulation and experimental results investigated the idea of the beam focusing using electromagnetic coupling improvement based on three dimensional periodic structures of circular split ring resonators and thin wires in microwave regime.

Keywords: Electromagnetic Coupling (EMC), Left-Handed Metamaterials (LHMM), Microstrip Patch Antenna (MPA), MM perfect lens, Negative Refractive Index (NRI), Nicolson-Ross-Weir (NRW), Circular Split Ring Resonators (CSRRs) and Thin Wires (TWs).

1. Introduction

Microstrip patch antennas offer an attractive solution to compact, conformal and low-cost designs of many wireless application systems [1]. It is well known that the gain of a single patch antenna is generally low and it can be increased by using array of patches or by reducing the surface wave, which can create ripples in the radiation pattern and hence reduce the main loop gain. Several methods have been proposed to reduce the effects of surface waves [2-8]. One approach suggested earlier is the synthesized substrate that lowers the effective dielectric constant of the substrate either under or around the patch [2-3]. Other approaches are to use parasitic elements [4-5] or to use a reduced surface-wave antenna [6-8]. During the last decade a metamaterial layer with negative refractive index has been developed to act as a lens [9]. This metamaterial (MM) lens can be placed in front of the patch antenna and due to the negative refractive index property of the MM, the radiated electromagnetic beam size reduces which results in a highly focused beam and hence the gain, directivity and radiation efficiency can be significantly improved [10, 11]. Metamaterials are artificial materials which exhibit their non-natural properties such as negative permittivity, negative permeability and negative refractive index (NRI) from

Cross ponding author; Tel. 01214144331, Fax.01214144291, e-mail: aaa365@bham.ac.uk; ghafourh@bham.ac.uk

physical dimensions and geometrical shapes rather that chemical composition [12-17]. Metamaterials which have simultaneous negative permittivity and negative permeability are called left-handed materials (LH-MM), in which the electric field *E*, the magnetic field *H*, and the wave vector *k* form a left-handed system.

Recently, several structures have been proposed which exhibit the LH-MM properties such as omega shape, spiral multi-split, fishnet, and S-shape [18-20]. After that many researchers have interested in investigating this artificial material, and several of them used the LH-MM to improve the properties of the microwave devices such as antennas and filters [21]. However, many papers have been published regarding the LH-MM integrated with antennas, and their properties have been analyzed [22-24]. Although other metamaterials such as frequency selective surface (FSS) and electromagnetic band gap (EBG) have been used to enhance the gain of an antenna [25-26], the NRI property of the LH-MM was exploited to improve the directivity and gain of the antennas [27-29]. In addition a metamaterial structure composed of copper grids with lattice was given by Stefan Enoch et al. for directive emission [30]. It was shown that the electromagnetic waves in the media can be congregated in a narrow rectangle area properly when applied to a monopole antenna; this structure can greatly improve the directivity of the antenna. Also, metamaterials have been designed and investigated in the THz frequency range for developing new THz devices such as antennas, filters, sensors, and absorbers [31-34].

In this paper, 3-D periodic structure consists of circular split ring resonators and thin wires (CSRRs/TWs) [35] is employed to improve the performance of a microstrip patch antenna operating at 10 GHz. The 3-D periodic structure is placed in front of the microstrip patch antenna and due to the Electromagnetic Coupling (EMC) property between the different unit cells forming the 3-D periodic structure and between the patch and the periodic structure, the radiated electromagnetic beam size reduces which results in a highly focused beam and hence the radiation parameters of the antenna such as gain, and directivity will be improved. Furthermore, the EMC impacts of using the CSRRs/TWs to improve the radiation and the impedance matching parameters of the patch antenna are considered as a preliminary phase in designing and testing CSRRs/TWs periodic structure with physical effective parameters to employ MM lens. This lens with physically realizable negative effective parameters (i.e. permittivity, permeability and index of refraction) can be used for the purpose of THz imaging; sensing and heart beat phasic measurement. In this work, a parametric analysis on a proposed patch antenna incorporated with CSRRs/TWs 3-D periodic structure employing EMC improvement in the near field area at the top of the patch and their impacts on the impedance matching and radiation parameters of the proposed antenna are studied. Both simulated and experimental results are verified.

This paper is organized as follows: Section 2 provides the design and simulation of the 10 GHz proposed patch antenna. Furthermore, this section includes; designs of a conventional line fed patch antenna at 10 GHz, frequency response of the CSRRs/TWs periodic structure, and parametric analysis of 10 GHz patch antenna incorporated with CSRRs/TWs 3-D periodic structure. The experimental validation of the proposed antenna is shown in section 3. Finally, the paper conclusion is given in section 4.

2. Analysis and Design of the Proposed Antenna

In order to investigate the idea of beam focusing using EMC improvement, a microstrip patch antenna operating at 10 GHz and a CSRR/TW unit cell resonating at the same frequency as that of the patch antenna are designed and simulated using CST microwave studio. The conventional patch antenna has a length, *L*, and width, *W*, of 8.6 mm and 11.86 mm, respectively, and is printed on a RT/Duroid 5880 substrate with a relative permittivity of ε_r = 2.2 and a thickness of *h*= 1.57 mm. The patch is fed by a 50 Ω microstrip line and is matched with quarter wavelength transformer which has a line length, L_T, and width,W_T, of 7mm and 0.3mm, respectively. The quarter wavelength transformer length and/or the patch width were optimized to give a good impedance matching. The size of the substrate $a \times b$ was calculated from the formula $(W + 6h) \times (L + 6h)$[36]. The conventional microstrip patch antenna (MSA) parameters such as gain, bandwidth, and directivity and radiation efficiency are calculated theoretically using cavity model [37]. The Directivity (*D*) is calculated as follow

$$D = \frac{2\left(\frac{4b^2\pi^2}{I_1\lambda_0}\right)}{1 + g_{12}} \quad (1)$$

$$I_1 = \int_0^{\pi} \sin^2\left(\frac{k_0 b\cos(\theta)}{2}\right)\tan^2(\theta)\sin(\theta)\,d\theta \quad (2)$$

And

$$g_{21} = \frac{1}{120\pi^2}\int_0^{\pi} \frac{\sin^2\left(\frac{\pi b cos(\theta)}{\lambda_0}\right)\tan^2\theta sin\theta\, J_0(\frac{2\pi a}{\lambda_0}sin\theta)}{G} d\theta \quad (3)$$

Where $J_o(x)$ is the zeroth-order Bessel function, k_o is the free space wave number equals $\lambda_0/2\pi$, a is the substrate length equals $W + 6h$, b is the substrate width equals $W + 6h$, and G is the radiation inductance $G = 1/R_r$ and R_r is the radiation resistance and is given by [37]

$$R_r = \frac{120\pi^2}{I_1} \quad (4)$$

The bandwidth BW of the MSA can also inversely proportional to its total quality factor Q_T and is given by [38]

$$BW = \frac{VSWR - 1}{Q_T\sqrt{VSWR}} \quad (5)$$

The total quality factor Q_T is given by [37]

$$\frac{1}{Q_T} = \frac{1}{Qr} + \frac{1}{Q_c} + \frac{1}{Qsw} + \frac{1}{Q_d} \quad (6)$$

Where Q_r Q_c, Q_{sw} and Q_d are the radiation, conductor, surface wave and dielectric quality factors, respectively. The relationship between *VSWR* and return loss S_{11} is as follows [38].

$$S_{11}(dB) = 20\log_{10}\left(\frac{VSWR}{VSWR - 1}\right) \quad (7)$$

The MSA radiation efficiency is given by [37]

$$e = \frac{Q_T}{Q_r} = \frac{Q_d Q_c Q_{sw}}{Q_{sw}Q_c Q_d + Q_{sw}Q_c Q_r + Q_{sw}Q_r Q_d + Q_r Q_d Q_c} \quad (8)$$

The gain G of the MSA is given by [37]

$$G = eD \quad (9)$$

The maximum gain of the conventional patch antenna is about 7 dB. Furthermore, the CSRR/TW unit cell is used to construct a 3-D EMC periodic structure which is then placed in front of the patch antenna with specific separation h_S as shown in Figs. 1 (a), 1 (b), 1 (c), and 1 (d) which illustrate the 3-D view, bottom view, top view and side view of the propose antenna, respectively. However, the 3-D CSRRs/TWs periodic structure is designed with specific periodicities of a_x, a_y, and a_z in *x*, *y*, and *z*, respectively to ensure a strong EMC coming out from the resonators formed by the CSRRs and the TWs which are constructing the 3-D periodic structure, and also, the separation distance h_S between the patch and the bottom side of the 3-D CSRRs/TWs periodic structure is designed properly to build a constructive electric and magnetic coupling between the patch and the CSRRs/TWs periodic structure. As a result the radiation and the impedance matching parameters of the proposed antenna can be improved as will be discussed in section 3. The detailed dimensions, the frequency response of the CSRR/TW unit cell constructing the EMC improvement structure will be given in the coming section. After that, the proposed antenna is simulated for different sizes of the 3-D CSRR/TW structure employing the EMC improvement structure at different separation h_S between the patch and the EMC periodic structure; as a result the optimized structure of the proposed antenna can be obtained.

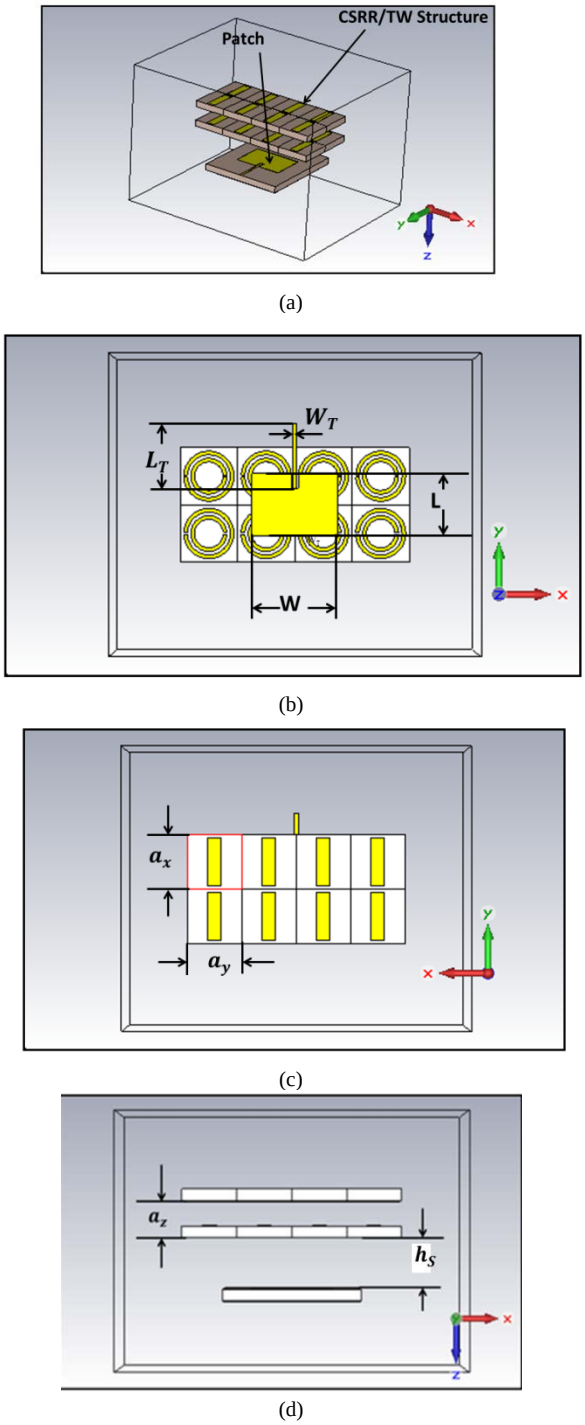

Fig. 1. The structure of the proposed antenna, (a) 3-D view, (b) bottom view, (c) top view and (d) side view.

2.1. Frequency Response of CSRR/TW unit cell resonating at 10 GHz

Here, a unit cell of CSRR/TW is designed and simulated in CST which when repeated in two dimensions; it may give us a good band pass response around the interesting frequency of 10 GHz [31]. The

dimensions of the 2-D CSRR/TW structure are optimized in order to give a strong EMC in a frequency range matched with the bandwidth of the patch antenna. The EMC improvement caused by the CSRRs/TWs periodic structure achieves an optimal beam focusing when it is integrated with the patch antenna. The CSRR is a copper layer with thickness t of 35 µm mounted on the top side of a RT/Duriod 5880 dielectric substrate with relative dielectric permittivity εr of 2.2 and height h = 1.57 mm, and the TW is mounted on the other side, i.e. the CSRR/TW structure is a double-sided process structure. The CSRR/TW unit cell is depicted in Fig. 2 was designed using the CST Microwave Studio to resonate at 10 GHz. The CSRR/TW parameters are: a=4.5 mm, g=0.3 mm, $r1i$=1 mm, $r1o$=1.4 mm, r_{2i}=1.8 mm, $r2o$=2.1 mm, L_{TW}= 4.2 mm. W_{TW}= 1 mm and t= 17 µm. The scattering parameters of the CSRR/TW unit cell are extracted as shown in Fig. 3 which illustrates that the CSRR/TW unit cell has a band pass frequency response with a transmission peak center frequency of 10 GHz. The CSRR/TW unit cell scattering parameters can be obtained by using boundary conditions of magnetic walls at the back and front sides since the magnetic field is polarized in the x-direction and also electric walls on the left and right sides as the electric field is polarized in the y-direction. The theoretical resonant frequency of the CSRR/TW unit cell is 10 GHz, according to the theories developed in [31], which is matched with the operating frequency of the patch antenna. The transversal periodicity is a = 4.5 mm, which is less than 1/8 of the free space wave length at resonance, which is used to construct the 3-D periodic structure to employ sub-wavelength EMC improvement.

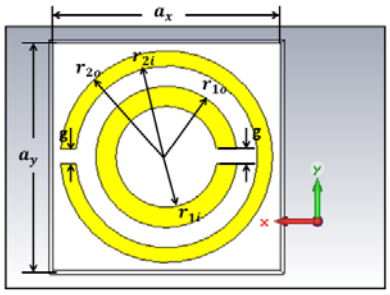

(a)

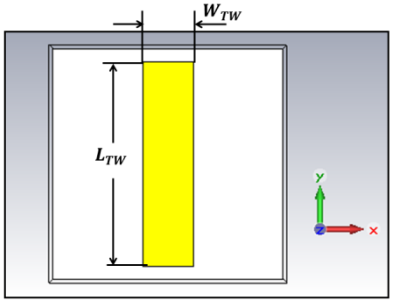

(b)

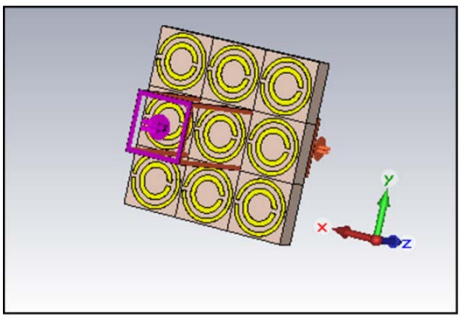

(c)

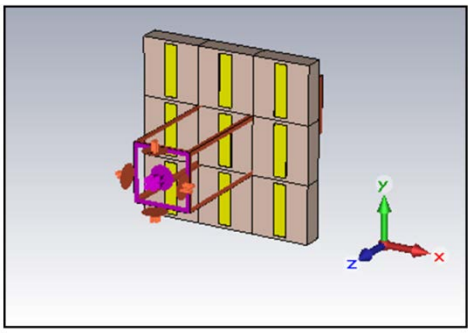

(d)

Fig. 2. The CSRR/TW unit cell structure (a) front view, (b) back view, (c) and (d) indicate 3-D view with boundary conditions of unit cells in x and y directions and the feeding source in the x-y plane.

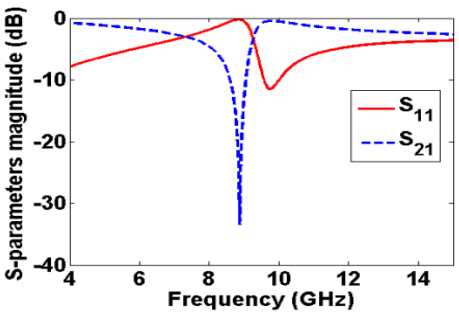

(a)

Fig.3. The 2-D CSRR/TWs infinite periodic structure scattering parameters with a pass band response around the fundamental resonance frequency of 10 GHz.

Figure 3 shows that, the CSRR/TW unit cell resonates at a fundamental frequency of 10 GHz and has a band pass response around the fundamental resonance frequency of 10 GHz. However, the bandwidths of the band pass of the CSRR/TW unit cell can be widened if the unit cell dimensions are increased and the first harmonic resonance of the CSRR/TW unit cell is chosen instead of the fundamental resonator. To do so, the dimensions of the CSRR/TW unit cell shown in Fig.2 are redesigned to has a first harmonic resonance around 10 GHz with a wider bandwidth. The CSRR/TW unit cell parameters are: a=8 mm, g=0.3 mm, $r1i$=2 mm, $r1o$=2.5 mm, $r2i$=3 mm, $r2o$=3.5 mm, L_{TW}= 7 mm. W_{TW}= 1 mm

and t= 17 µm. The scattering parameters of the CSRRs/TWs unit cell have been extracted. Fig. 4 shows that the CSRR/TW unit cell has a band pass frequency response with a center frequency of 10 GHz. It is clear from Figs. 3 and 4 that, since the CSRR/TW 2-D infinite periodic structure has a good band pass response, the CSRR/TW structure allows the radiated electromagnetic (EM) waves from the patch to transmitted through it and improved by the EMC property between the different resonators of such structure and between the structure and the patch. Although, the CSRR/TW negative effective parameters are tried to be extracted (the results not shown here) from the s-parameters by the procedure of Nicolson-Ross-Weir (NRW) algorithm and unambiguity presented in [39, 40], this procedure results in a non-physical response. To overcome this problem, the EMC property can be used to demonstrate the radiation and impedance matching improvements of the proposed antenna rather than the NRI property of the MM lens.

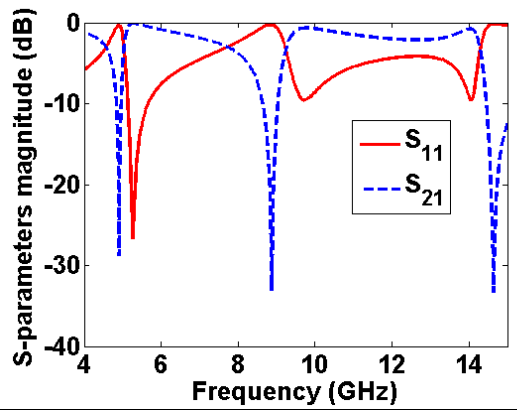

(a)

Fig. 4. The 2-D CSRRs/TWs infinite periodic structure scattering parameters with a band pass response around the first harmonic resonance frequency of 10 GHz.

The impact of the CSRRs/TWs infinite periodic structure truncation on the frequency response of the CSRRs/TWs structure is considered. It is impossible to use infinite periodic structure in our application of incorporating the patch antenna with the CSRRs/TWs EMC improvement structure, since the patch antenna has a finite patch length of $\lambda/2$ and patch width which determines the antenna impedance matching. This means that we have a finite CSRR/TW size which can be identified as function of the patch dimensions and the resonance wavelength to make sure that the antenna impedance matching occurs and at the same time the CSRRs/TWs structure has a good scattering parameters around the resonance frequency and the CSRRs/TWs homogeneity [40] is still satisfied to avoid the destroy of the radiated waves and to make a constructive EM coupling between the patch and the CSRRs/TWs structure. For example in the direction of the antenna patch length L which is the y- axis as shown in Fig. 1, the infinite periodicity is truncated at two unit cells of cell size a=8 mm, and this number of cells satisfies the CSRRs/TWs homogeneity at the operating wavelength which is 30 mm at 10 GHz, since at this frequency, the ratio λ/a will be approximately 4, which means that, two unit cells are required to cover the patch of effective length $L=\lambda/2$ of 15 mm in the direction of the patch length. This means that, there will be approximately $\lambda/4$ wave propagating across each CSRR/TW unit cell which is not bad related to the periodic structure homogeneity condition. Furthermore, it is good if we can increase the number of CSRR/TW unit cells per wavelength greater than 8, and this can be done by taking a unit cell of 4.5 mm size and has a fundamental resonance frequency of 10 GHz, this approach is suggested and unfortunately a less gain improvement is achieved (the results not shown here). So to tackle the tradeoff between the periodic structure homogeneity and the antenna performance improvement, a consistent homogeneity factor of 4 is chosen. However, if the number of cells in the direction of the patch length is increased, it will affect the impedance matching of the antenna and the return loss is increased as will be illustrated in the next section (see Fig. 6 (a) for a CSRRs/TWs structure size of $3 \times 3 \times 2$), so two unit cells are the optimum number in the y-direction. For the number of cells in x-direction aligned to the patch width which, different sizes of 2, 3 and 4 are used which fully cover the patch and even the whole antenna substrate. While in the z-direction, the periodicity of the CSRRs/TWs structure is truncated at two unit cells, since more cells in such direction will cause impedance mismatching.

To verify the above explanation of the infinite periodicity truncation of the CSRRs/TWs periodic structure, three different 3-D periodic structures with truncated periodicity of sizes $2 \times 2 \times 2$, $3 \times 3 \times 2$, and $4 \times 2 \times 2$, in addition to one 2-D periodic structure with infinite periodicity are designed and simulated in CST software. The scattering parameters of the periodic structures with infinite and truncated periodicities are traced as shown in Fig.5. It is clear that the return loss and the transmission characteristics of the 3-D truncated periodic structures are better than that of the 2-D periodic structure with infinite periodicity. In case of the truncated 3-D CSRRs/TWs periodic structures, the EMC is improved strongly in the propagation direction due to inter-layer coupling. Moreover there is EMC improvement in the transverse directions due to the coupling between the resonators of the different unit cells, while in case of the infinite 2-D periodic structure; there is only improvement in the transverse directions. Figure 5 illustrates that, the infinite periodicity truncation of the periodic structure does not destroy the band pass frequency response and hence the EMC properties of the CSRRs/TWs structure around 10 GHz. In addition, the

results showed a shift in the resonance frequency toward the lower frequency for the 3-D periodic structure with truncated periodicity compared with the two periodic structures with infinite periodicity. This frequency shift will be compensated when the 3-D periodic structure is integrated with the patch antenna and make the proposed antenna resonate at 10 GHz because of the capacitive gap between the patch and the 3-D periodic structure.

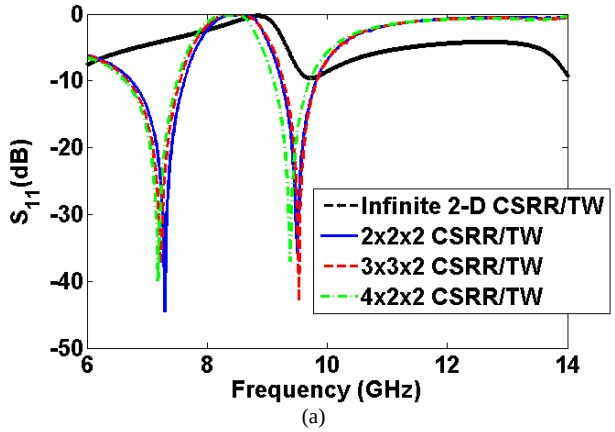

(a)

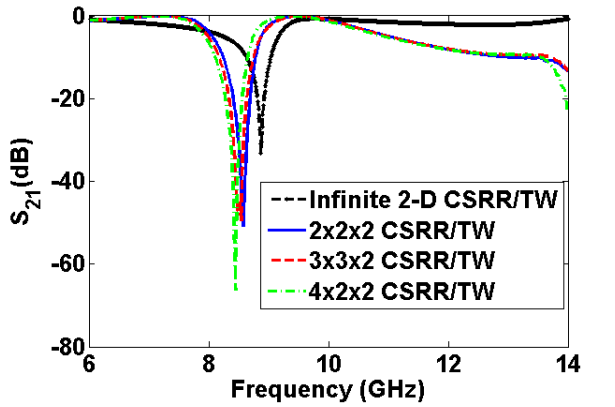

(b)

Fig.5. Magnitude of the scattering parameters of the 3-D periodic structure with truncated periodicity by building the CSRRs/TWs periodic structure from 3-D structure with finite sizes of $2 \times 2 \times 2$, $3 \times 3 \times 2$ and$4 \times 2 \times 2$ (a) S_{11}, and (b) S_{21}.

2.2. Design and Simulation of 10 GHz Patch Antenna incorporated with CSRRs/TWs Periodic Structure in Front of the Patch

Here, the proposed patch antenna incorporated with CSRRs/TWs periodic structure is analyzed, simulated and optimized using CST software. The proposed antenna is operating at 10 GHz and the CSRRs/TWs periodic structure is optimized to present a strong EMC between the patch and the CSRRs/TWs periodic structure in a wideband around the 10 GHz. The antenna is optimized by changing the size of the CSRRs/TWs periodic structure and the separation between the CSRRs/TWs periodic structure and the patch. Figures 6 (a) and 6 (b) show the return loss and the radiation gain at 10 GHz of the proposed antenna at 10 mm separation distance h_s between the patch and the CSRRs/TWs periodic structure bottom side and at different CSRRs/TWs periodic structure sizes.

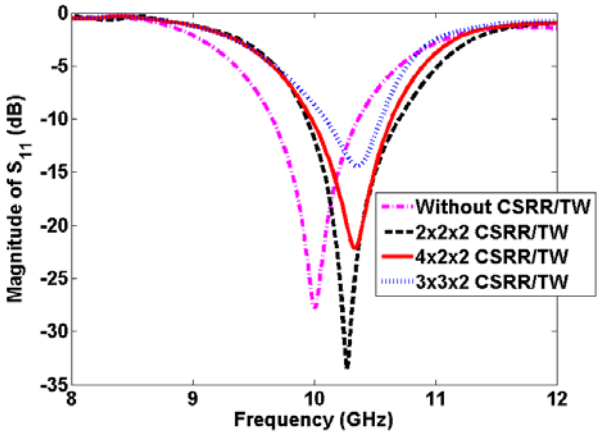

(a)

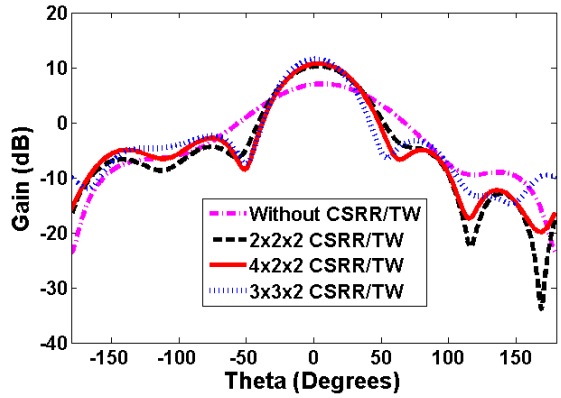

(b)

Fig. 6. The simulated return loss (a) and the simulated gain at 10 GHz of the proposed antenna with and without CSRRs/TWs periodic structure of different sizes and at 10 mm separation distance h_s between the patch and the CSRRs/TWs periodic structure.

Furthermore, the effect of the patch and CSRRs/TWs periodic structure separation on the radiation and impedance matching parameters are studied by fixing the size of the CSRRs/TWs periodic structure at 3×3×2 in *x*, *y* and *z* direction, respectively and changing the separation distance h_s from 6 mm to 12 mm by step size of 2 mm. It is clear that the proposed antenna is optimized at a separation distance of 10 mm. The return loss and the radiation gain for the proposed antenna at different patch and CSRRs/TWs periodic structure separation and at a 3×3×2 periodic structure size is plotted as shown in Figs. 7 (a) and 7 (b). However, the magnitude of the near electric and magnetic fields of the proposed antenna with and without CSRRs/TWs periodic structure at 10 GHz are plotted as shown in Fig. 8. It is clear that, by placing a CSRRs/TWs periodic structure of size 3×3×2 and

identifying the convergence mesh criteria in the CST, the electric field *E* magnitude is improved from 29788 v/m to 37996 v/m and the magnetic field *H* strength is slightly improved from 76.4 A/m to 77.1 A/m and the field is focused above the patch around the center of the CSRRs/TWs periodic structure which claims that the CSRRs/TWs periodic structure employing a EMC improvement. It is important to notice that, the shown number for the *E* and *H* fields are just to clarify the improvement in the near field of the patch antenna which occurs due to the CSRRs/TWs periodic structure and these numbers may be changed slightly if the numbers of meshes in the CST are changed.

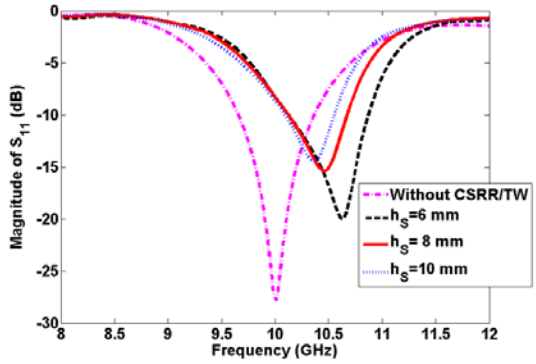

(a)

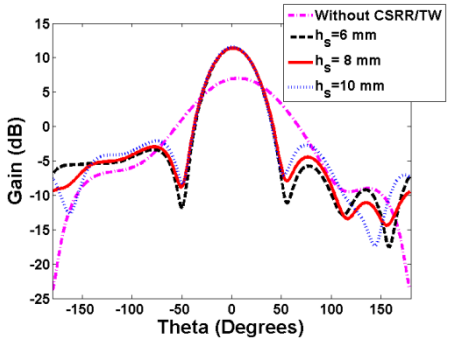

(b)

Fig. 7. The simulated return loss (a) and the simulated gain at 10 GHz of the proposed antenna with and without CSRRs/TWs periodic structure of size 3x3x2 and different separation distances h_s between the patch and the CSRRs/TWs periodic structure.

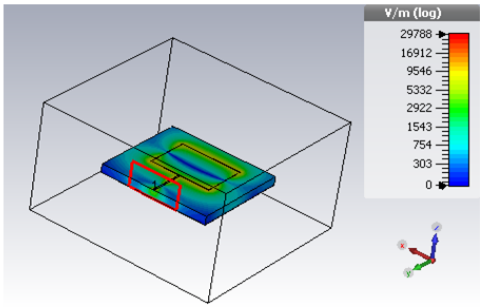

(a)

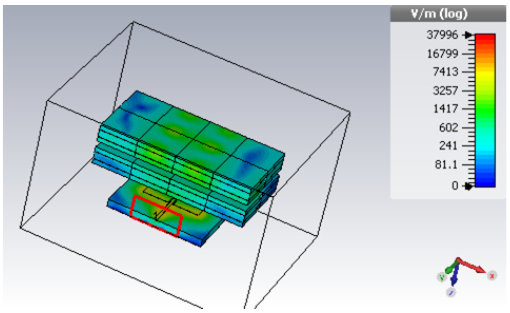

(b)

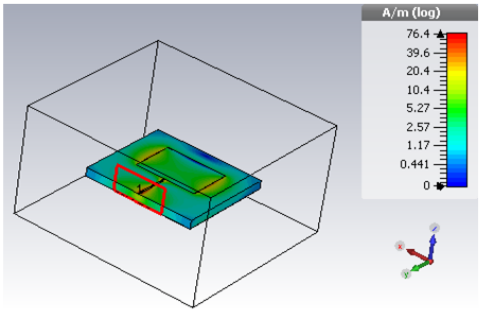

(c)

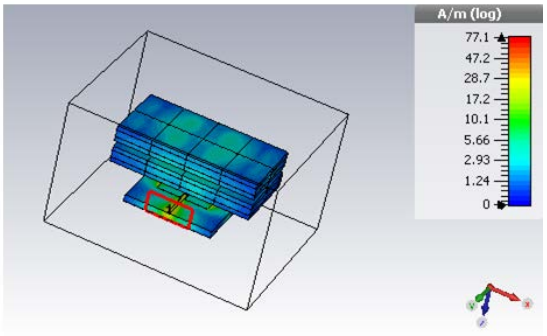

(d)

Fig. 8. Near field of the proposed antenna without and with periodic structure at 10 GHz, (a) *E*-field without periodic structure, (b) *E*-field with periodic structure, (c) *H*-field without CSRRs/TWs periodic structure and (d) *H*-field with CSRRs/TWs periodic structure.

It is clear from Figs. 6 that, as the size of the CSRRs/TWs periodic structure increases, the gain increases, and the beam area is reduced, while the return loss increases (decreases with negative values), and the bandwidth is increased. As the CSRRs/TWs periodic structure is added the losses of the antenna increases, so the total quality factor decreases and hence according to equation (5) given above, the bandwidth increases. Furthermore, according to equations (6, 8 and 9), the gain improves for the antenna with CSRRs/TWs periodic structure although the losses increases, because the beam becomes more directive due to the EMC improvement

caused by the CSRRs/TWs periodic structure and hence the directivity *D* increases. The increase in directivity *D* is more than the reduction in the antenna efficiency due to the losses presented by the CSRRs/TWs periodic structure, so the antenna gain increases. Furthermore, according to equation 7, the reason behind the reduction in the return loss of the proposed antenna comes from the change in input impedance which determines the *VSWR* of the antenna. The antenna input impedance is changed due to the magnetic and the electric coupling between the patch and the CSRRs/TWs periodic structure which result in adding a reactance term to the antenna input impedances, as a result the resistive part of the antenna input impedance may be become more dominant and hence impedance matching is occurred and the return loss is improved as in the case of CSRRs/TWs periodic structure of 2×2×2 size or it may happen the opposite situation such as in the remaining sizes of the CSRRs/TWs periodic structures as shown in Fig. 6 (a). In one word, it can be said that, the input impedance and hence the return loss of the antenna is affected dramatically when the CSRRs/TWs periodic structure is added and a great effort should be done to impedance match the antenna by choosing the optimal CSRRs/TWs periodic structure size and the separation distance between the patch and the CSRRs/TWs periodic structure. However, it is obvious that, the optimum CSRRs/TWs periodic structure has a sized of 3×3×2 and the optimum separation distance between the patch and the CSRRs/TWs periodic structure is 10 mm. For the optimized proposed antenna, the simulated gain is improved from 7 dB to 11.6 dB, the band width is improved from 700 dB to 900 dB, while the return loss increases and the antenna is less matched. In addition, for a patch antenna with a CSRRs/TWs periodic structure of size 2×2×2 separated from the patch at a distance h_S of 10 mm, the return loss is improved from -27 dB to -35 dB as shown in Fig. 6 (a), while the beam area is reduced from 75 degrees to 41 degree as shown in Fig. 6 (b). However, it should be noticed from Fig. 6 and 7 that, as the size of the CSRRs/TWs periodic structure employing the EMC improvement increases, the return loss increases and the antenna matching becomes worst due to the loading effect of the CSRRs/TWs periodic structure which affects directly the input impedance of the antenna, so to avoid this problem a compromise between the return loss and the gain of the antenna should be done to obtain a good matching and a high gain at the same time.

3. Fabrication and Measurement

For experimental validation, the proposed antenna resonating at 10 GHz as well as the CSRRs/TWs periodic structure have been fabricated as shown in Fig. 9. The fabrication is done using wet etching technique on a RT/Duroid 5880 substrate for both the patch antenna and the CSRRs/TWs periodic structure with a relative permittivity of ε_r = 2.2 and a thickness of h= 1.57 mm. The return loss, S_{11} for the simulated and the fabricated antenna with and without CSRRs/TWs periodic structure is shown in Fig. 10. Furthermore, the effect of the separation distance between the patch and the CSRRs/TWs periodic structure of size 3x3x2, and the effect of the CSRRs/TWs periodic structure size at fixed separation h_S of 8 mm, on the impedance matching of the antenna are illustrated as shown in Fig. 10(a) and Fig 10 (b), respectively. The measured bandwidth of the patch antenna with and without CSRRs/TWs periodic structure is approximately the same which is around 400 MHz. However, the measured return loss of the 10 GHz proposed antenna incorporated with CSRRs/TWs periodic structure placed on the patch at a separation distance of 8 mm and of size 3×3×2 is improved from -13 dB to -30 dB.

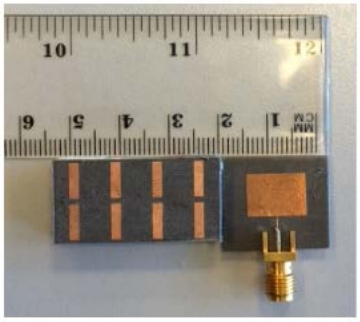

(a)

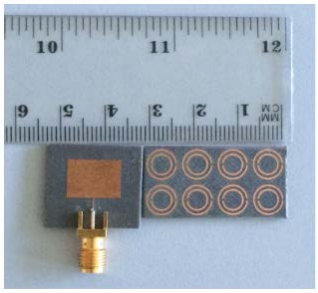

(b)

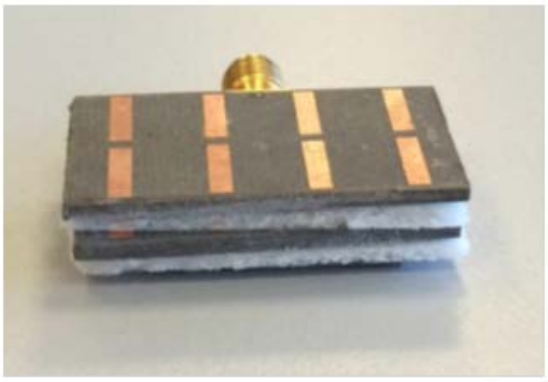

(c)

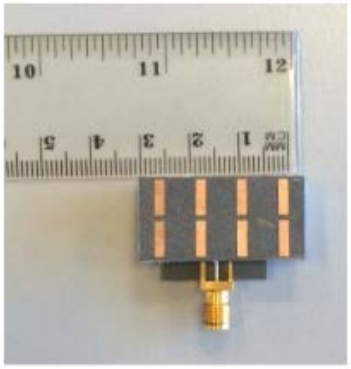

(d)

Fig. 9. The fabricated antenna, (a) conventional patch and top view of CSRRs/TWs 2-D periodic structure of size 4×4×2, (b) conventional patch and bottom view of CSRRs/TWs 2-D periodic structure, 3-D view of the proposed antenna, and (d) top view of the proposed antenna incorporated with CSRRs/TWs periodic structure.

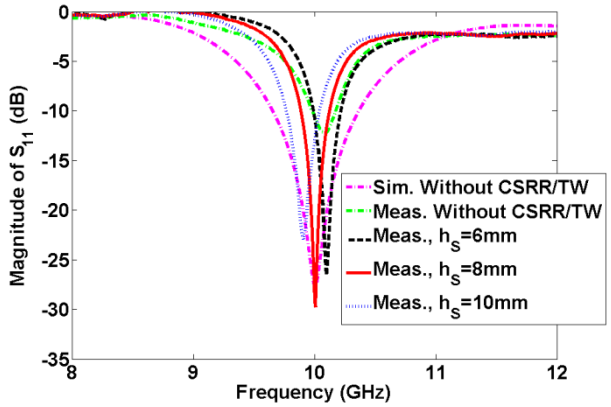

(a)

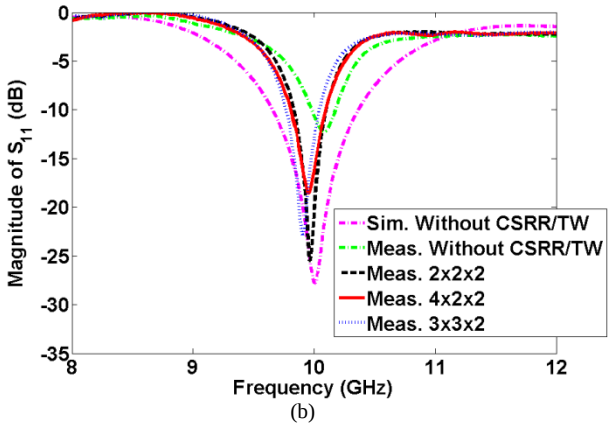

(b)

Fig. 10. The measured and simulated return loss of the proposed antenna with and without CSRRs/TWs periodic structure (conventional): (a) at different separation between the CSRRs/TWs periodic structure and the patch and 3x3x2 CSRRs/TWs periodic structure size, and (b) at different CSRRs/TWs periodic structure sizes and separation distance of 8 mm between the patch and the CSRRs/TWs periodic structure.

Furthermore, both *E*-plane and *H*-plane radiation patterns at 10 GHz proposed antenna with and without periodic structure are measured for different periodic structure of sizes 4×2×2 and 3×3×2 and fixed separation h_S of 10 mm between the patch and the bottom side of the periodic structure as shown in Fig. 11. However, the simulated *E*-plane and *H*-plane radiation patterns at 10 GHz proposed antenna with and without periodic structure are plotted on the same figure.

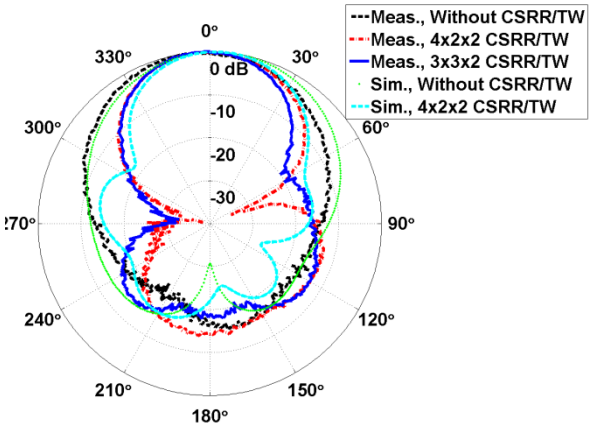

(a)

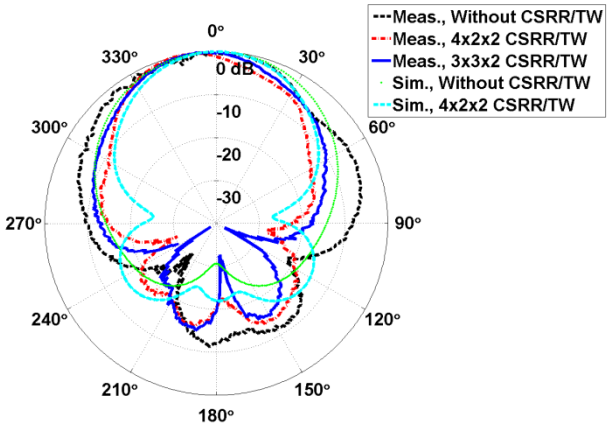

(b)

Fig. 11. Measured and simulated radiation pattern at 10 GHz of the proposed antenna with and without CSRRs/TWs periodic structure for different CSRRs/TWs periodic structure sizes, (a) *E*-plane and (b) *H*-plane and fixed separation h_S of 10 mm between the patch and the CSRRs/TWs periodic structure ns

The results showed a good agreement between the simulated and the measured results and that the radiation beam in both *E*-plane and *H*-plane become more focused as the CSRRs/TWs periodic structure is placed as the top of the patch. To verify the ideal that as the beam becomes more focused and hence the gain of the antenna is improved, the gain versus frequency for the proposed antenna with and without CSRRs/TWs periodic structure for different periodic structure sizes of 3×3×2 and 4×2×2 and fixed separation of 10 mm between the patch and the

periodic structure bottom side is plotted as shown in Fig. 12.

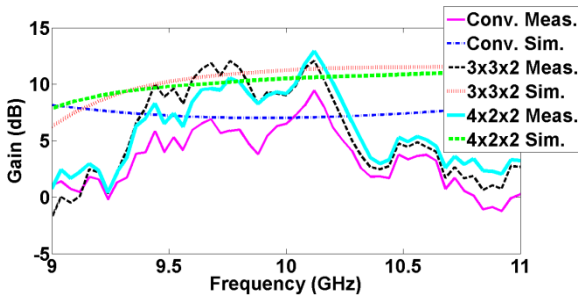

Fig.12. Comparison between the measured and the simulated gains of the proposed antenna with and with CSRRs/TWs periodic structure of different sizes and fixed separation h_s of 10 mm between the patch and the CSRRs/TWs periodic structure.

It is clear from Fig. 12 that, the simulated gain of the proposed antenna incorporated with CSRRs/TWs periodic structure of 3×3×2 size is improved from 7 dB to 11.6 dB inside the bandwidth of the antenna, at the same time the measured gain is also improved approximately with the same figures. The gain versus frequency graph of Fig. 12 shows that the measured and the simulated gain of the proposed antenna are roughly closed inside the antenna bandwidth but with little bit fluctuation due to the measurement errors and the misalignment of the placement of the CSRRs/TWs periodic structure above the patch. However, as the periodic structure size increases, the gain of the proposed antenna increases, because the periodic structure congregates more EM waves from the patch radiated waves and the beam becomes more focus.

4. Conclusion

In this paper, the performance of a 10 GHz patch antenna is greatly improved by beam focusing when it is integrated with a 3-D CSRRs/TWs periodic structure employing EMC improvement. The CSRRs/TWs periodic structure was suspended above the patch antenna through bears made of foam; the CSRRs/TWs periodic structure focused the radiated EM waves of the patch antenna in a narrow area. A 2-D infinite periodicity CSRR/TWs structure is designed and simulated in CST software and the scattering parameters are extracted, the results illustrated that the CSRRs/TWs periodic structure has a band pass scattering parameters. In addition, the infinite periodicity truncation of the CSRRs/TWs periodic structure is also studied by designing and simulated 3-D periodic structure with finite sizes of 2×2×2, 3×3×2, and 4×2×2. The results showed that, the periodic structure truncation has no significant impacts on both the periodic structure band pass scattering parameters and homogeneity.

The proposed antenna has been designed and optimized in CST software, the antenna bandwidth is improve and the return loss generally increases. The results showed that, as the CSRRs/TWs periodic structure is added the losses of the antenna increases, so the total quality factor decreases and hence the bandwidth increases. The change in the impedance matching and hence the return loss is because of the capacitive and inductive coupling between the patch and the CSRRs/TWs periodic structure. The optimized radiation properties of the proposed patch antenna have been obtained through the justification of the patch and the periodic structure separation and the dimensions of the 3-D CSRRs/TWs periodic structure. These improvements in the antenna parameters validate the proposed concept of beam focusing using 3-D periodic structure of CSRRs/TWs employing the EMC improvement, without modifying significantly in the matching methodology of the patch antenna. Furthermore, we have demonstrated the validity of the above properties by CST software EM simulator and experimentally at 10 GHz and showed that, at this frequency the antenna gain, has improved by 4.6 dB, while the beam width is reduced from 75 degrees to 41 degrees which validate the concept of beam focusing using CSRRs/TWs periodic structure. The measured and the simulated results showed an improvement in the return loss by about -20 dB for the antenna incorporated with CSRRs/TWs periodic structure of size 2×2×2 although it increases when 3×3×2 and 4×2×2 periodic structure sizes are used. This improvement is due to the reactance coming out from the electric and the magnetic coupling between the patch and the CSRRs/TWs periodic structure and the coupling between the different parts of the CSRRs/TWs periodic structure itself which result in a reactance term added to the antenna input impedance. As a future work, the idea of gain improvement of the patch antenna incorporated with the CSRRs/TWs periodic structure can be extended to THz frequency rang to be used for short distance wireless communication link, particularly in the biomedical application and inside the satellite to reduce the wiring complexity of the satellite system and. However, the CSRRs/TWs periodic structure can replace the bulky silicon lens used in the THz optical antennas to focus the radiated beam and improve the antenna gain. Also, the CSRRs/TWs periodic structure will be redesigned to have tens of thousands of unit cells to be employed as MM lens for beam focusing and hence gain improvement purposes of the radiated wave from the patch and optical antennas for medical applications [41, 42]. The effective parameters of the CSRRs/TWs will be extracted such that they have a physical and unambiguity response.

References

[1] R. Collin, Field theory of guided waves. New York: McGraw-Hill, 1960.

[2] G. Gauthier, A. Courtay and G. Rebeiz, 'Microstrip antennas on synthesized low dielectric-constant substrates', IEEE Transactions on Antennas and Propagation, vol. 45, no. 8, pp. 1310-1314, 1997.

[3] J. Colburn and Y. Rahmat-Samii, 'Patch antennas on externally perforated high dielectric constant substrates', IEEE Transactions on Antennas and Propagation, vol. 47, no. 12, pp. 1785-1794, 1999.

[4] D. Kokotoff, R. Waterhouse, C. Birtcher and J. Aberle, 'Annular ring coupled circular patch with enhanced performance', Electron. Lett., vol. 33, no. 24, p. 2000, 1997.

[5] R. Rojas and K. Lee, 'Surface wave control using nonperiodic parasitic strips in printed antennas', IEE Proceedings - Microwaves, Antennas and Propagation, vol. 148, no. 1, p. 25, 2001.

[6] A. Bhattacharyya, 'Characteristics of space and surface waves in a multilayered structure (microstrip antennas)', IEEE Transactions on Antennas and Propagation, vol. 40, no. 8, pp. 1231-1240, 1990.

[7] D. Jackson, J. Williams, A. Bhattacharyya, R. Smith, S. Buchheit and S. Long, 'Microstrip patch designs that do not excite surface waves', IEEE Transactions on Antennas and Propagation, vol. 41, no. 8, pp. 1026-1037, 1993.

[8] M. Khayat, J. Williams, D. Jackson and S. Long, 'Mutual coupling between reduced surface-wave microstrip antennas', IEEE Transactions on Antennas and Propagation, vol. 48, no. 10, pp. 1581-1593, 2000.

[9] J. Pendry, 'Negative Refraction Makes a Perfect Lens', Phys. Rev. Lett., vol. 85, no. 18, pp. 4166-4169, 2000.

[10] Z. Weng, N. Wang, Y. Jiao and F. Zhang, 'A directive patch antenna with metamaterial structure', Microwave and Optical Technology Letters, vol. 49, no. 2, pp. 456-459, 2006.

[11] Y. Liu and X. Zhao, 'Enhanced patch antenna performances using dendritic structure metamaterials', Microwave and Optical Technology Letters, vol. 51, no. 7, pp. 1732-1740, 2009.

[12] D. Smith, W. Padilla, D. Vier, S. Nemat-Nasser and S. Schultz, 'Composite Medium with Simultaneously Negative Permeability and Permittivity', Phys. Rev. Lett., vol. 84, no. 18, pp. 4184-4187, 2000.

[13] D. Smith and N. Kroll, 'Negative Refractive Index in Left-Handed Materials', Phys. Rev. Lett., vol. 85, no. 14, pp. 2933-2936, 2000.

[14] R. Shelby, 'Experimental Verification of a Negative Index of Refraction', Science, vol. 292, no. 5514, pp. 77-79, 2001.

[15] A. Grbic and G. Eleftheriades, 'Periodic analysis of a 2-D negative refractive index transmission line structure', IEEE Transactions on Antennas and Propagation, vol. 51, no. 10, pp. 2604-2611, 2003.

[16] L. Chen, S. He and L. Shen, 'Finite-Size Effects of a Left-Handed Material Slab on the Image Quality', Phys. Rev. Lett., vol. 92, no. 10, 2004.

[17] V. Veselago, 'THE ELECTRODYNAMICS OF SUBSTANCES WITH SIMULTANEOUSLY NEGATIVE VALUES OF ε AND μ', Sov. Phys. Usp., vol. 10, no. 4, pp. 509-514, 1968.

[18] Majid, H. A., Abd Rahim, M. K., & Masri, T. (2009). Microstrip antenna's gain enhancement using left-handed metamaterial structure. Progress In Electromagnetics Research M, 8, 235-247.

[19] K. Alici, F. Bilotti, L. Vegni and E. Ozbay, 'Optimization and tunability of deep subwavelength resonators for metamaterial applications: complete enhanced transmission through a subwavelength aperture', Opt. Express, vol. 17, no. 8, p. 5933, 2009.

[20] K. Alici and E. Ozbay, 'Characterization and tilted response of a fishnet metamaterial operating at 100 GHz', Journal of Physics D: Applied Physics, vol. 41, no. 13, p. 135011, 2008.

[21] M. Gil, J. Bonache, J. Selga, J. Garcia-Garcia and F. Martin, 'High-pass Filters Implemented by Composite Right/Left Handed (CRLH) Transmission Lines Based on Complementary Split Rings Resonators (CSRRs)', PIERS Online, vol. 3, no. 3, pp. 251-253, 2007.

[22] K. Buell, H. Mosallaei and K. Sarabandi, 'A substrate for small patch antennas providing tunable miniaturization factors', IEEE Transactions on Microwave Theory and Techniques, vol. 54, no. 1, pp. 135-146, 2006.

[23] K. Alici and E. Ozbay, 'Electrically small split ring resonator antennas', J. Appl. Phys., vol. 101, no. 8, p. 083104, 2007.

[24] A. Alu, F. Bilotti, N. Engheta and L. Vegni, 'Subwavelength, Compact, Resonant Patch Antennas Loaded With Metamaterials', IEEE Transactions on Antennas and Propagation, vol. 55, no. 1, pp. 13-25, 2007.

[25] A. Pirhadi, F. Keshmiri, M. Hakkak and M. Tayarani, 'ANALYSIS AND DESIGN OF DUAL BAND HIGH DIRECTIVE EBG RESONATOR ANTENNA USING SQUARE LOOP FSS AS SUPERSTRATE LAYER', PIER, vol. 70, pp. 1-20, 2007.

[26] Y. Lee, J. Yeo, K. Ko, R. Mittra, Y. Lee and W. Park, 'A novel design technique for control of defect frequencies of an electromagnetic bandgap (EBG) superstrate for dual-band directivity enhancement', Microwave and Optical Technology Letters, vol. 42, no. 1, pp. 25-31, 2004.

[27] A. Erentok, P. Luljak and R. Ziolkowski, 'Characterization of a volumetric metamaterial realization of an artificial magnetic conductor for antenna applications', IEEE Transactions on Antennas and Propagation, vol. 53, no. 1, pp. 160-172, 2005.

[28] S. Burokur, M. Latrach and S. Toutain, 'Theoretical Investigation of a Circular Patch Antenna in the Presence of a Left-Handed Medium', Antennas and Wireless Propagation Letters, vol. 4, no. 1, pp. 183-186, 2005.

[29] B. Li, B. Wu and C. Liang, 'STUDY ON HIGH GAIN CIRCULAR WAVEGUIDE ARRAY ANTENNA WITH METAMATERIAL STRUCTURE', PIER, vol. 60, pp. 207-219, 2006.

[30] S. Enoch, G. Tayeb, P. Sabouroux, N. Guérin and P. Vincent, 'A Metamaterial for Directive Emission', Phys. Rev. Lett., vol. 89, no. 21, 2002.

[31] M. El-Nawawy, A. A. Allam and A. Korzec, 'The Design of a 0.35THz Microstrip Patch Antenna on LTCC Substrate', EEE, vol. 1, no. 1, pp. 1-4, 2011.

[32] J. Turpin, J. Bossard, K. Morgan, D. Werner and P. Werner, 'Reconfigurable and Tunable Metamaterials: A Review of the Theory and Applications', International Journal of Antennas and Propagation, vol. 2014, pp. 1-18, 2014.

[33] I. Vendik, O. Vendik, M. Odit, D. Kholodnyak, S. Zubko, M. Sitnikova, P. Turalchuk, K. Zemlyakov, I. Munina, D. Kozlov, V. Turgaliev, A. Ustinov, Yeonsang Park, Jinyun Kihm and Chang-Won Lee, 'Tunable Metamaterials for Controlling THz Radiation', IEEE Transactions on Terahertz Science and Technology, vol. 2, no. 5, pp. 540-549, 2012.

[34] R. ZIOLKOWSKI, 'Metamaterial-Based Antennas: Research and Developments', IEICE Transactions on Electronics, vol. 89-, no. 9, pp. 1267-1275, 2006.

[35] J. Woodley, M. Wheeler and M. Mojahedi, 'Left-handed and right-handed metamaterials composed of split ring resonators and strip wires', Physical Review E, vol. 71, no. 6, 2005.

[36] Kamtongdee, C., & Wongkasem, N. (2009, May). A novel design of compact 2.4 GHz microstrip antennas. In Electrical Engineering/Electronics, Computer, Telecommunications and Information Technology, 2009. ECTI-CON 2009. 6th International Conference on (Vol. 2, pp. 766-769). IEEE.

[37] Bancroft, R. (2009). Microstrip and printed antenna design. The Institution of Engineering and Technology.

[38] H. Pues and A. V Capelle, “Accurate transmission-line model for the rectangular microstrip antenna, “Proc. IEEE, vol. 131, no.6, pp. 334-340, December 1984.

[39] X. Chen, T. Grzegorczyk, B. Wu, J. Pacheco and J. Kong, 'Robust method to retrieve the constitutive effective parameters of metamaterials', Physical Review E, vol. 70, no. 1, 2004.

[40] Arslanagic, S., Hansen, T. V., Mortensen, N. A., Gregersen, A. H., Sigmund, O., Ziolkowski, R. W., & Breinbjerg, O. (2013). A review of the scattering-parameter extraction method with clarification of ambiguity issues in relation to metamaterial homogenization. Antennas and Propagation Magazine, IEEE, 55(2), 91-106.

[41] Y. Kurzweil-Segev, M. Brodsky, A. Polsman, E. Safrai, Y. Feldman, S. Einav and P. Ben Ishai, 'Remote Monitoring of Phasic Heart Rate Changes From the Palm', IEEE Transactions on Terahertz Science and Technology, vol. 4, no. 5, pp. 618-623, 2014.

[42] Sun, M., Chen, Z. N., Tanoto, H., Wu, Q. Y., Teng, J. H., & Yeap, S. B. (2010, December). Design of Continuous-Wave Photomixer Driven Terahertz Dipole Lens Antennas. In APSIPA Annual Summit and Conference (pp. 14-17).